Green Chemistry

PAPER

View Article Online
View Journal | View Issue

Cite this: *Green Chem.*, 2025, **27**, 3207

A techno-economically feasible and sustainable C-lignin biorefinery†

Pu Wang,[a,c] Shuizhong Wang,[d] Shihao Su,[c] Dexin Zhang,[a,c] Yuhe Liao,[e] Guoyong Song *[d] and Lei Wang *[b,c]

Received 1st December 2024,
Accepted 18th February 2025

DOI: 10.1039/d4gc06090c

rsc.li/greenchem

C-lignin, a homo-biopolymer, has great potential as a feedstock for biorefineries that convert it into high value-added products, for example, catechol as a precursor of pharmaceuticals. In this study, we conducted a techno-economic analysis (TEA) and life cycle assessment (LCA) of a conceptual biorefinery where waste castor seed coats are converted into high value-added products, including pulp, catechol, oligomers, and propylene. After several rounds of optimization through scenario studies, with the incorporation of combined heat and power (CHP) and pressure swing adsorption (PSA) systems, as well as importing heat and electricity instead of using natural gas, bio-catechol achieves a minimum selling price (MSP) of $2.02 per kg, 23% lower than the market price, and a carbon footprint of 1.58 kg CO_2 eq. per kg, 72% lower than that of fossil derived catechol. In addition, the use of district heat co-generated by natural gas or biogas CHP plants can further reduce the GWP of bio-catechol, but with trade-offs in other environmental impacts. Nevertheless, this study has proposed potentially economically viable and sustainable C-lignin biorefineries with products to replace fossil derived catechol.

Green foundation

1. C-lignin, a homo-biopolymer, has great potential as a feedstock for biorefineries that convert it into high value-added products, such as catechol. This study proposed a conceptual biorefinery where waste castor seed coats are converted into high value-added products, including pulp, catechol, oligomers, and propylene.
2. A techno-economic analysis and a life cycle assessment were conducted, and the results indicate that the proposed biorefinery is a potentially economically viable and sustainable C-lignin biorefinery with products to replace fossil derived catechol.
3. The implementation of biomethanol, renewable energy, and green hydrogen could further reduce the carbon footprint of C-lignin derived catechol.

1. Introduction

With the rapid development of the world economy and population growth, a large amount of organic solid waste is generated globally with lignocellulosic biomass waste as a substantial proportion.[1–4] It has been reported that 5.28 billion tonnes of crop waste were generated globally in 2020, with an annual production of about 740 million tonnes of crop straw and 200 million tonnes of forestry biomass in China.[5,6] The improper disposal of this large volume of lignocellulosic waste could result in environmental contamination and health risks, for example, pollution caused by open-air combustion.[7] Besides, this lignocellulosic waste is a renewable and "carbon neutral" resource with great potential as a feedstock for a wide range of high-value products (energy, chemicals, and materials) that replace conventional fossil fuel-based materials, thereby reducing greenhouse gas emissions and playing an important role in the future bioeconomy.[8–10]

The major components of lignocellulosic biomass are cellulose, hemicellulose, and lignin.[11] Biorefining is a process that utilizes these major components to produce bio-fuels, materials and high-quality fine chemicals. While cellulose and hemicellulose have been mainly hydrolyzed into sugars for

[a]College of Environmental and Resource Sciences, Zhejiang University, Hangzhou 310058, Zhejiang, China
[b]Zhejiang Key Laboratory of Low-Carbon Intelligent Synthetic Biology, Westlake University, Hangzhou, Zhejiang 310030, China. E-mail: wang_lei@westlake.edu.cn
[c]Institute of Advanced Technology, Westlake Institute for Advanced Study, Hangzhou, Zhejiang 310024, China
[d]State Key Laboratory of Efficient Production of Forest Resources, Beijing Key Laboratory of Lignocellulosic Chemistry, Beijing Forestry University, Beijing 100083, China. E-mail: songg@bjfu.edu.cn
[e]Guangzhou Institute of Energy Conversion, Chinese Academy of Sciences, Guangzhou 510640, Guangdong, China

† Electronic supplementary information (ESI) available. See DOI: https://doi.org/10.1039/d4gc06090c

fuels and chemicals, lignin has been underutilized as a solid fuel and its economically feasible value-added applications are still lacking.[12] Recently, there have been a number of studies proposing lignin-first biorefineries that extract lignin from lignocellulosic biomass and convert it through depolymerization, oxidative or reductive conversions into valuable chemicals such as eugenol, vanillin, guaiacol, phenol, polyethylene terephthalate, benzene, *etc*.[13–17] Catechyl lignin (C-lignin), a uniform and linear biopolymer, is considered an ideal lignin due to its efficient depolymerization into catechol derivatives, demonstrating high potential for biorefinery.[18] For example, several reports have indicated that the supported metal catalysts, such as Ru/C,[19,20] Pd/C,[21,22] Pt/C,[19] Cu-PMO,[23] Ni/C,[24,25] and Ru/ZnO/C ,[26] catalyzed hydrogenolysis of isolated C-lignin samples from vanilla and *Euphorbiaceae* seed coats, which give catechol derivatives with end-chains. Nar *et al.* indicated that C-lignin extracted from vanilla (*V. planifolia*) seed coats can be used to fabricate carbon fiber.[27] Zhao *et al.* indicated that the microbial conversion of extracted C-lignin from vanilla, Euphorbia, and candlenut shells to polyhydroxyalkanoates (PHAs) showed superior performance in terms of biodegradability compared to fossil-based plastics.[28]

In addition to technological development in the field of biorefining, assessments using techno-economic and life cycle assessments coupled with process simulations using Aspen Plus® have been applied.[29,30] The application of these analyses can identify the advantages and disadvantages of the technology developed, as well as the major contributors to cost and environmental impacts. For example, Bartling *et al.*[31] suggested that priority should be given to efforts to reduce reductive catalytic fractionation (RCF) operating pressure and hence capital expenditure. Arts *et al.*[32] concluded that the level of solvent recycling is a key parameter affecting the economic viability and sustainability of an RCF biorefinery process. Liao *et al.*[33] concluded that an economically competitive process with a lower carbon footprint could be achieved that converts lignin to phenol *via* reductive catalytic fractionation (RCF) funneling. For C-lignin, Mabrouk *et al.*[34] performed a techno-economic analysis (TEA) and concluded that catechols from olive tree prunings are economically competitive, whilst Montazeri *et al.*[35] reported that tertbutyl catechol (TBC) from candlenut shells has a slight advantage in carbon footprint (~2% less) compared to the fossil product. However, systematic TEA and LCA assessments of C-lignin biorefineries based on process modelling are still lacking.

In this study, we proposed a conceptual C-lignin based multi-product biorefinery plant and assessed it from both TEA and LCA perspectives for the first time. In addition, we also proposed different scenarios by integrating renewable energy sources, paving the way for this C-lignin biorefinery towards sustainability in the future.

2. Methodologies

2.1 Process description and simulation

The biorefinery process was designed to convert waste castor seed coats into pulp, oligomers, propylene, and catechol *via* lignin extraction, catalytic hydrogenolysis, and product separation. The conceptual biorefinery plant was designed to include eight areas, which are feedstock pretreatment (A100), catalytic hydrogenolysis (A200), oligomer extraction (A300), dealkylation (A400), product separation (A500), combined heat and power (A600), storage (A700), and the cooling water system (A800), as shown in Fig. 1a. Mass and energy flows were modelled using Aspen Plus® V12. The processing capacity is assumed to be 1500 kg h^{-1} for castor seed coats, reflecting a conceptual plant built next to a castor seed oil production site in Inner Mongolia with a castor seed treatment capacity of 60 000 t y^{-1}.[36,37] Operating assumptions and mass balance for principal reaction sections were adopted from previously published work and described in the ESI (Table S2).†[38–40] The capital costs for A700 and A800 were scaled up/down based on the information from NREL reports.[38,39] In the pretreatment section, castor seed coats are extracted using methanol at a mass ratio of 1 : 4.4 (feedstock to methanol)[33] and 70 °C under 1.3–1.5 bar, yielding C-lignin intermediates fed to the hydrogenolysis section (Fig. 1b). In the hydrogenolysis section, the reactor is pressurized to H_2 (3 MPa) at room temperature. The C-lignin intermediates are converted to propanolcatechol, propylcatechol, catechol, and oligomers using a Ru/C catalyst and under 200 °C, after methanol recovery and oligomer separation, propylcatechol is dealkylated to catechol. The product stream is then distilled to yield catechol as the main product and propanolcatechol and propylene as co-products (Fig. 1c). The process description and modelling details are documented in the ESI.†

2.2 Techno-economic analysis

The economic performance of this conceptual plant was measured using the minimum selling price (MSP, $ per kg) of bio-catechol using the discounted cash flow rate of return analysis (DCFROR). Costs for DCFROR were capital expenditure (CAPEX) and operating expenses (OPEX), including materials, energy, and labor costs. The mass and energy flow data obtained from the process simulation were used to estimate the capital costs. The reference year of the plant is 2023. The overall principles of MSP calculations were adopted from NREL reports and values were documented in the ESI Excel.†[38–40]

In the CAPEX estimation, the costs of tanks, drums, pumps, and basic heat exchangers were estimated using Aspen Plus ACCE (Aspen Capital Cost Estimator) after considering the corrosion issues. For specific equipment, such as catalytic hydrogenolysis reactor, dealkylation reactor, and filter press, as well as sectors, such as CHP, storage and cooling water systems, their purchase costs were estimated with an "nth plant" assumption as shown in the following exponential expression using (eqn (1)).[38]

$$\text{New Cost} = \text{Base Cost}\left(\frac{\text{New Size}}{\text{Base Size}}\right)^{n} \quad (1)$$

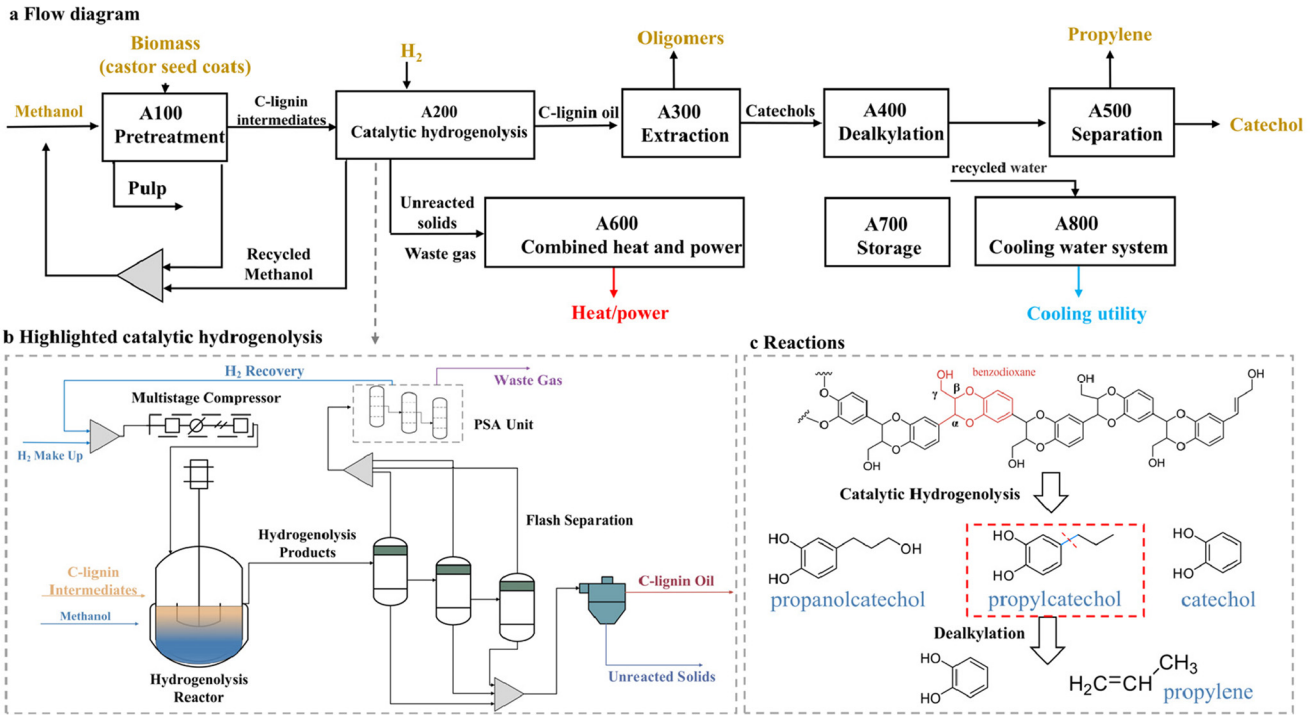

Fig. 1 The proposed integrated C-lignin biorefinery: (a) flow diagram of processes with materials (brown), heat (red) and cooling (blue) flows. (b) Highlighted catalytic hydrogenolysis. (c) Sketch of reactions.

where n is a characteristic scaling exponent based upon production capacity, such as flow or heat duty. n is selected within the range of 0.6–0.7 according to the equipment type and 0.6 for cost estimation of sectors.[41]

The obtained purchase costs were adjusted to the reference year (2023) with Chemical Engineering's Plant Cost Index (CEPCI) using (eqn (2)).[42] Once the total purchased equipment costs (TPEC) were determined, scaled, and time-corrected, an equipment installation factor was applied to estimate the total installed capital cost (TIC) using (eqn (3)).

$$\text{Eqpt. Cost in 2023} = \text{Eqpt. Cost}\left(\frac{\text{2023 Cost Index Value}}{\text{Base year Cost Index Value}}\right) \quad (2)$$

$$\text{TIC} = f_{\text{instal.}} \times \text{TPEC} \quad (3)$$

Finally, we applied China Location Factors to adjust the TIC to reflect the effects of local material price, labor and manufacturing cost using (eqn (4)).[43]

$$\text{TIC in China} = f_{\text{location}} \times \text{TIC} \quad (4)$$

2.3 Life cycle assessment (LCA)

Following the ISO 14040 series, LCA was performed in four steps: goal and scope definition, life cycle inventory (LCI), life cycle impact assessment (LCIA), and interpretation of results.[44,45]

2.3.1 Goal and scope definition. The goal of this study was to quantify the environmental impacts of bio-catechol produced from C-lignin in castor seed coats and compare them with those of fossil-derived catechol (*via* phenol hydroxylation). The functional unit was set as 1 kg of catechol. The system boundary was "cradle to gate", including pretreatment, catalytic hydrogenolysis, oligomer extraction, dealkylation, and product separation. Chemical (*e.g.*, methanol, hydrogen, and *n*-hexane) production and transportation (50 km by truck) are included in the system boundary, as well as catalysts. The feedstock was a castor seed oil product waste stream and therefore its production and transportation were not included in the system boundary. Infrastructure and land use were also excluded from the system boundary with a 2% cut-off rule applied. The system expansion for surplus electricity replacing the grid and the economic allocation between multiple biomass products were used. The pulp and C-lignin intermediates including isolated C-lignin and extracts were outputs of the pretreatment area (A100). Hence, the emissions associated with pretreatment were allocated between the products of pretreatment. The emissions associated with the remaining areas of this process were allocated between oligomers, propylene and catechol.

2.3.2 Life cycle inventory (LCI). For the conceptual biorefinery and its scenarios, mass, energy and emissions flows were derived from our in-house Aspen Plus® models. For fossil-derived catechol production, data were obtained from a manufacturer located in Anhui Province with a capacity of 15 000 t y^{-1}.[46] Background data were from the Ecoinvent® v3.3 database embedded in SimaPro® (v9.0) software. Life cycle inventories for the 5% Ru/C catalyst and green hydrogen were

established based on production processes (ESI Tables S14 and S15†). The transportation distance for chemicals was assumed to be 50 km *via* a lorry.

2.3.3 Life cycle impact assessment (LCIA). The ReCiPe2016 (H) method was applied for impact assessment where 18 environmental impact categories were assessed, including global warming potential (GWP, kg CO_2 eq.), stratospheric ozone depletion (ODP, kg CFC11 eq.), ionizing radiation (IRP, kBq Co-60 eq.), ozone formation-human health (HOFP, kg NO_x eq.), fine particulate matter formation (PMFP, kg PM 2.5 eq.), ozone formation-terrestrial ecosystems (EOFP, kg NO_x eq.), terrestrial acidification (TAP, kg SO_2 eq.), freshwater eutrophication (FEP, kg P eq.), marine eutrophication (MEP, kg N eq.), terrestrial ecotoxicity (TETP, kg 1,4-DCB), freshwater ecotoxicity (FETP, kg 1,4-DCB), marine ecotoxicity (METP, kg 1,4-DCB), human carcinogenic toxicity (HTPc, kg 1,4-DCB), human non-carcinogenic toxicity (HTPnc, kg 1,4-DCB), land use (LOP, m^2 a crop eq.), mineral resource scarcity (SOP, kg Cu eq.), fossil resource scarcity (FFP, kg oil eq.), and water consumption (WCP, m^3) (ReCiPe 2016).[47]

2.4 Scenario setting

To assess the effects of various process designs on the economic and environmental performance of the conceptual plant, scenarios were set as follows:

- Baseline scenario: castor seed coats were converted into high value-added products, including pulp, oligomers, bio-catechol, and propylene without incorporating CHP or PSA systems.
- Scenario 1: we incorporated the CHP system (A600) into combust waste streams with imported natural gas as an additional fuel.
- Scenario 2: we integrated the PSA subsystem into A200 to recycle excess hydrogen back to the catalytic hydrogenolysis reactor.
- Scenario 3: we eliminated natural gas imports and imported heat as steam supplied by natural gas co-generation units, boilers and industrial furnaces instead.
- Scenarios 4 and 5: the heat (steam) source was switched to natural gas and biogas co-generation plants, respectively.
- Scenarios 6, 7 and 8: fossil-based methanol, electricity and hydrogen were replaced by renewable resources step by step.

3. Results and discussion

3.1 Baseline scenario (S0): mass and energy balance

The composition of the castor seed coat and elemental analysis results are demonstrated in Table 1. The mass balance analysis of the castor seed coat indicates a relatively high product yield of 78.27% including 72.93% pulp, 4.00% oligomers, 1.07% bio-catechol, and 0.27% propylene. Solid waste and waste gas emissions account for the rest 21.73% of mass (Fig. 2a). The results of elemental analysis of the extract-free

Table 1 Feedstock composition (wt%) and elemental analysis (%)

Sample	Available C-lignin[a]	Cellulose	Hemicellulose	Extractives	Moisture	Ash	Other components[b]
Castor seed coat	4.60	14.09	8.58	13.95	7.00	2.80	48.98

	C	H	N	S	O
Extractive-free castor seed coat	50.26	5.70	0.94	0.11	42.99
Isolated C-lignin	59.43	6.26	0.38	—	33.93

[a] This value was calculated based on quantitative ^{13}C NMR spectroscopy characterization of the sample obtained from the methanol extraction. [b] This value was obtained by the lignin quantification method from the NREL report using acid hydrolysis.[49] The amount of other components equals to that of lignin extracted by acid hydrolysis minus C-lignin, containing G-type and S-type lignin, as well as a small amount of lipids.

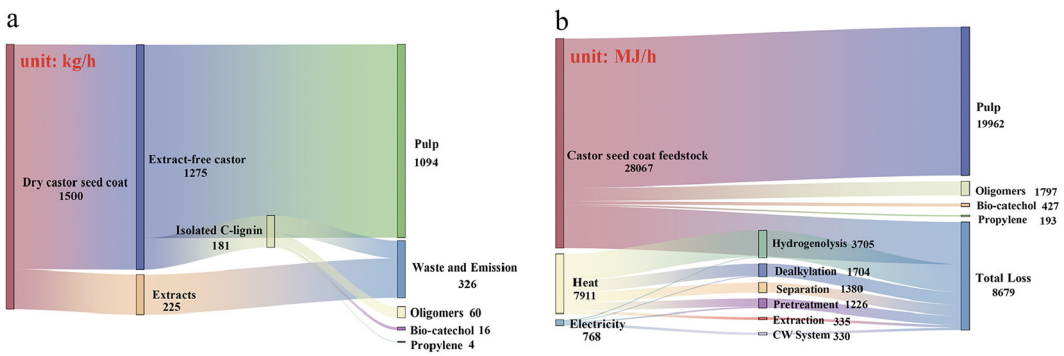

Fig. 2 (a) Mass balance of feedstock (kg h^{-1}) and (b) energy balance (MJ h^{-1}) of the conceptual biorefinery (baseline scenario).

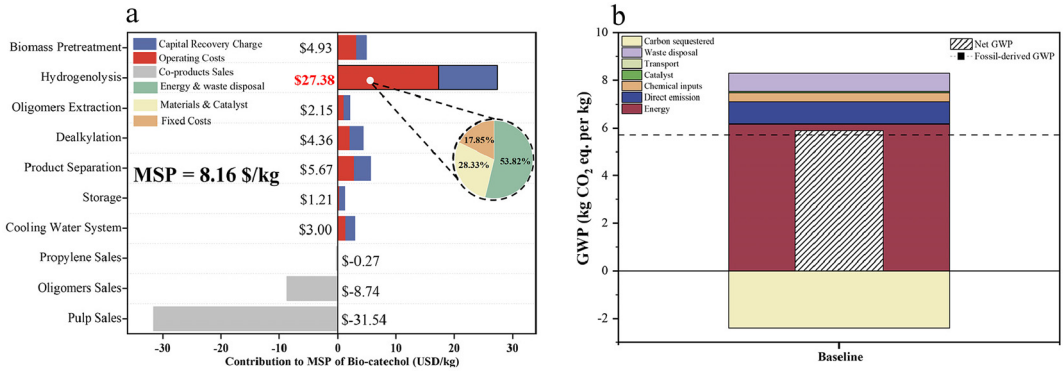

Fig. 3 TEA and LCA results of bio-catechol production in the baseline scenario. (a) Breakdown of MSP. (b) Breakdown of GWP with that of fossil-derived catechol indicated by the dashed line.

castor seed coat and isolated C-lignin are presented in Table 1, which are the basis for estimating the higher heating value (HHV) of the extract-free castor seed coat and pulp.[48] The energy inputs to the system (HHV) are from the castor seed coat, thermal energy (steam), and electrical energy, contributing 28 066.68 MJ h^{-1} (76.83%), 7910.92 MJ h^{-1} (21.53%), and 768.30 MJ h^{-1} (2.09%), respectively. The catalytic hydrogenolysis reaction in A200 accounts for the highest energy demand (42.64%) due to high temperature and pressure. The energy flow balance analysis indicates that energy efficiencies of 79.73% based on the castor seed coat and 60.90% for the entire system are achieved (Fig. 2b). Energy loss is due to heat and electricity consumption during the catalytic hydrogenolysis and emissions from solid waste landfilling and exhaust gas into the environment.

3.2 Baseline scenario (S0): TEA and LCA

According to the results of TEA, the MSP of bio-catechol produced by this process is $8.16 per kg, higher than the average market price of fossil-derived catechol ($2.63 per kg).[50] Fig. 3a illustrates the contributors to the MSP of bio-catechol in each process area, where positive values are associated costs and negative values are revenues of product sales. Among all process areas, A200 makes the highest contribution to the positive values of MSP ($27.38 per kg), which accounts for 56.21% of the total costs including capital costs and OPEX. Notably, OPEX contributes more significantly than the capital recovery charge at $17.29 per kg, accounting for 63.15% of the total cost of A200. Within OPEX, energy consumption and waste disposal are dominant at $9.30 per kg, accounting for 53.82%. Within energy consumption, 52.90% is for maintaining the reaction at 200 °C, while 45.03% is for methanol recovery. Within power consumption, pumps and hydrogen compressors are the major consumers. For capital recovery charge, catalytic hydrogenolysis under high temperature and pressure conditions resulted in a relatively high reactor capital expenditure.[51] The solid waste including unreacted C-lignin intermediates and extractives as well as the lost catalysts was assumed to be landfilled with a cost of $0.26 per kg.[52] The direct emission of exhaust gases including methane and methanol is not permitted; therefore, it was assumed to be disposed of by flaring.[53] Overall, though the annual revenue from the sale of multiple co-products (pulp, oligomers, and propylene) offsets the total cost by $40.55 per kg, bio-catechol produced is not economically competitive with fossil-derived catechol.

According to LCA results (Fig. 3b), the contribution analysis reveals that the consumption of fossil energy and electricity accounts for approximately 6.17 kg CO_2 eq. per kg and 74.32% of the positive score, followed by direct emissions at 0.94 kg CO_2 eq. per kg as the second largest contributor (11.31%). The GWP of bio-catechol is 5.90 kg CO_2 eq. per kg, higher than 5.72 kg CO_2 eq. per kg of fossil-derived catechol but lower than those of other phenolic products derived from lignin, *e.g.*, tert-butyl catechol (TBC, 13.40 kg CO_2 eq. per kg).[35]

The analysis of the baseline scenario reveals that it is neither economically feasible nor sustainable. The disposal of solid waste with an HHV of 17.65 MJ kg^{-1} and the flaring of exhaust gas with an HHV of 35.51 MJ kg^{-1} results in the loss of embedded energy; therefore, a CHP system was incorporated in Scenario 1 for the utilization of these waste streams.

3.3 Scenario analysis

3.3.1 The incorporation of CHP. In S1, where CHP was incorporated into combust waste streams, the MSP of bio-catechol is $4.51 per kg, 44.73% lower than the $8.16 per kg MSP in the baseline, though still higher than the price of fossil-derived products ($2.63 per kg). In S1, the capital recovery charge is estimated to be the most significant contributor to the MSP at $25.99 per kg, accounting for 57.39% of the total positive value. This is followed by materials, catalysts, and waste disposal costs at $8.62 per kg (19.04%); fixed costs at $6.59 per kg (14.54%); and energy costs at $4.09 per kg (9.03%). Compared to the baseline, S1 has higher capital recovery costs ($25.99 per kg *vs.* $20.54 per kg) due to the incorporation of the CHP system (Fig. 4a). The major cost contributors to the capital recovery charge are A200 (49.12% for S0 and 35.01% for S1) and A600 (28.7% for S1). The distribution of TIC aligns with findings from other studies analyzing similar

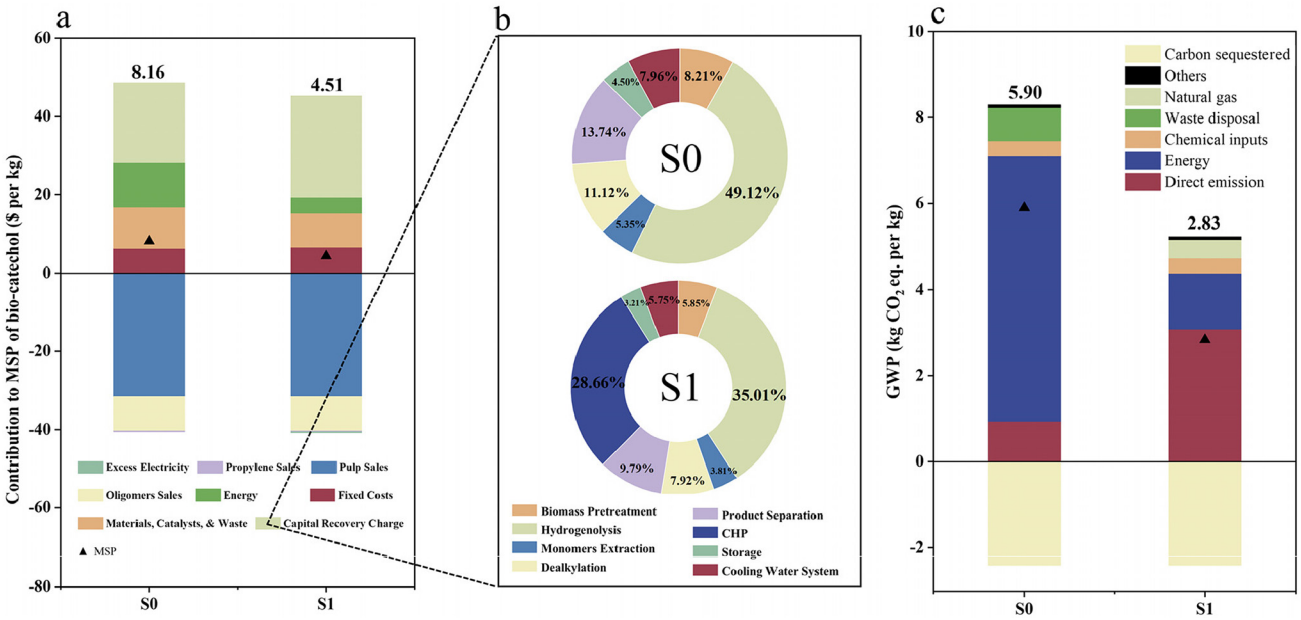

Fig. 4 TEA and LCA results of bio-catechol production in S0 and S1. (a) Breakdown of MSP. (b) Breakdown of total capital recovery charge based on different processes. (c) Breakdown of GWP based on types of inputs.

technologies (Fig. 4b).[31] However, energy costs ($4.09 per kg *vs.* $11.37 per kg) are lower because the combustion of waste streams provides energy to the system and eliminates partial waste treatment expenses ($4.19 per kg). In addition, natural gas is supplied to the CHP system to fulfill the demand for energy and electricity demand, with surplus electricity assumed to be sold back to the grid, generating credits as a negative score. Overall, the incorporation of CHP enhanced the economic feasibility of the system.

With regards to the sustainability assessment (Fig. 4c), the GWP of bio-catechol production is 2.83 kg CO_2 eq. per kg, which is 52.03% lower than the 5.90 kg CO_2 eq. per kg in the baseline scenario. Compared with the baseline where energy consumption is the major contributor (74.32%), direct emissions in S1 are the main contributor (3.08 kg CO_2 eq. per kg, 58.96%), followed by energy use (1.30 kg CO_2 eq. per kg, 24.86%), natural gas production (0.43 kg CO_2 eq. per kg, 8.17%), chemicals (0.35 kg CO_2 eq. per kg, 6.68%), and others (0.07 kg CO_2 eq. per kg, 1.33%). Transitioning from S0 to S1 results in a significant surge in GWP caused by direct emissions, from 0.94 to 3.08 kg CO_2 eq. per kg. The primary reason for this surge is that the import of natural gas in S1 causes additional direct emission. However, the solid waste and exhausted gas including methane and methanol generated in the catalytic hydrogenolysis area are combusted in the CHP system, resulting in the reduction in GWP caused by energy use, which can offset the surge in GWP caused by direct emission. Therefore, the integration of the CHP system plays a positive role in reducing carbon emissions. Overall, the incorporation of the CHP system can improve both the economic feasibility and GWP of this process.

3.3.2 The incorporation of PSA and the switch of the energy source. Within the OPEX of S1, the cost of hydrogen accounts for $0.60 million per y. To further improve the economic performance of the conceptual biorefinery, PSA was incorporated into S2. The MSP of bio-catechol in S2 is $3.41 per kg, lower than that of S1 ($4.51 per kg). In S2, the capital recovery cost is the largest contributor to the MSP at $26.45 per kg, accounting for 59.95% of the positive score, followed by material and catalyst costs at $6.90 per kg (15.65%), fixed costs at $6.67 per kg (15.13%) and energy costs at $4.09 per kg (9.27%). Compared to S1, S2 has higher capital recovery costs ($26.45 per kg *vs.* $25.99 per kg) due to the inclusion of PSA in A200. Meanwhile, the material costs ($6.90 per kg *vs.* $8.62 per kg) are lower due to the recycling of hydrogen, despite the additional import of natural gas. However, the GWP of bio-catechol in S2 (3.18 kg CO_2 eq. per kg) is higher than that in S1 (2.83 kg CO_2 eq. per kg). This is because the recycling of hydrogen and methanol reduces the environmental impact of their production by 2.65%, but this eliminates the energy from their combustion as fuel and increases the demand for and combustion of natural gas by 9.45%, thereby increasing the overall GWP by 6.80%. Therefore, the inclusion of PSA could improve economic feasibility, but at the cost of an increase in GWP.

Switching natural gas imports to steam and grid electricity reduced the MSP from $3.41 in S2 to $2.02 in S3, lower than the market price of $2.63 per kg (Fig. 5a). As shown in Fig. 5b, the capital recovery charge associated with CHP (A600) decreases from 28.08% to 22.10% due to the reduction in fuel burned on-site and the resulting reduction in CAPEX from $3.50 million to $2.54 million. A sensitivity analysis was per-

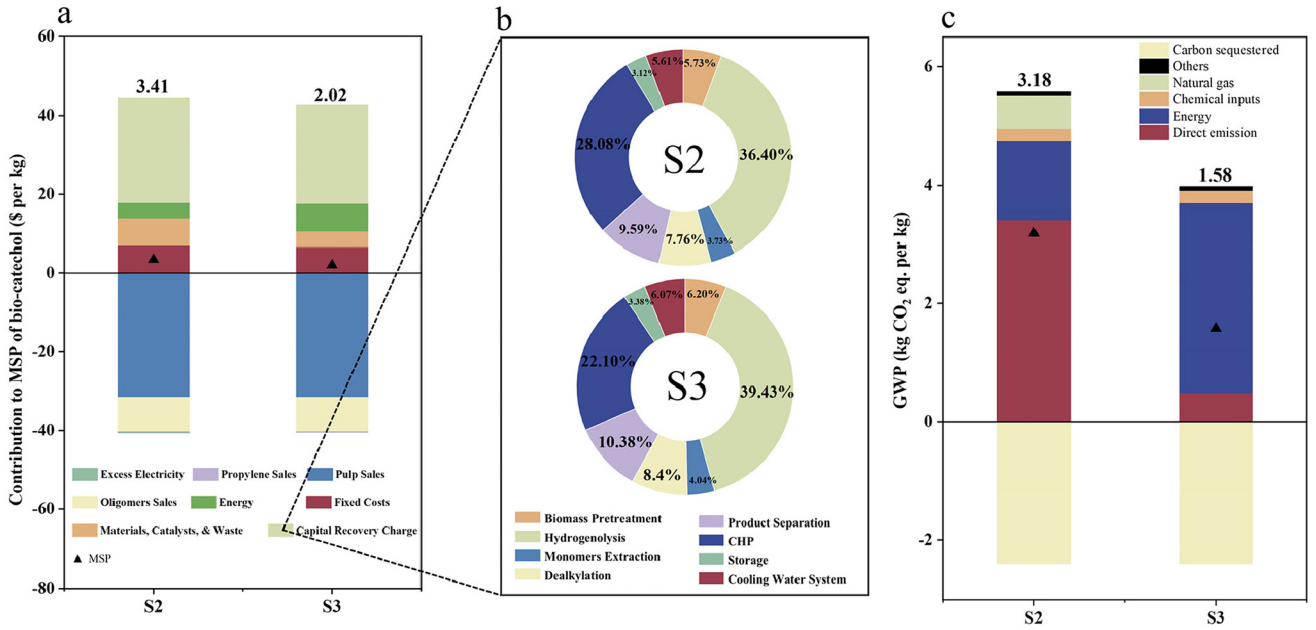

Fig. 5 TEA and LCA results of bio-catechol production in S2 and S3. (a) Breakdown of MSP. (b) Breakdown of total capital recovery charge based on different processes. (c) Breakdown of GWP based on types of inputs.

formed to evaluate the influence of process parameters (*e.g.*, C-lignin extraction yield and hydrogenolysis time), cost assumptions (*e.g.*, capital and operating expenditure and product prices) and economic parameters. The results (Fig S7†) show that the MSP of bio-catechol is most affected by the moisture content of pulp and capital expenditure in A200. From a sustainability perspective (Fig. 5c), the GWP is reduced from 3.18 to 1.58 kg CO_2 eq. per kg due to the reduction in direct emissions from natural gas combustion, despite the increase in emissions from imported energy.

As summarized in Table 2, S0 has a higher GWP than fossil-derived catechol production and an MSP above the market price. From the baseline (S0) to S3, after incorporating CHP and PSA and changing the energy supply mode, the energy efficiency and GWP of the system are gradually improved, while the economic performance fluctuates (Fig. 6a). Although all optimized scenarios have a lower GWP than fossil-based production, only S3 is economically feasible. Regarding the results of the full LCA analysis (Fig. 6b and Tables S3–S7†), S0 has higher GWP, ODP, MEP, and HTPnc than fossil-derived catechol due to landfilling of solid waste. However, fossil-derived catechol has higher impacts on IRP, TETP, FETP, METP, and HTPc due to the use of phenol and hydrogen peroxide. In S1, the CHP combustion of solid waste offsets part of the energy demand and therefore reduces the demand for natural gas and the environmental impacts associated with its production and use. In S2, the HTPnc and WCP metrics are lower; however, the other environmental metrics increase by 10% to 20% due to the additional import of natural gas. From S2 to S3, most of the environmental metrics increased due to the import of electricity except for GWP and FFP. This is due to higher boiler efficiency in the industry (approx. 90%) than our onsite natural gas boiler (approx. 85%).[54]

Compared to S3, S1 and S2 demonstrate better sustainability, except for GWP and fossil resource scarcity, but have less advanced economic feasibility. Trade-offs emerged between economic feasibility and sustainability, and between environmental performance. Effective decision-making requires a thorough understanding of these trade-offs.

Furthermore, in order to demonstrate opportunities for sustainability improvement, additional scenarios were conducted, such as the use of heat from natural gas co-generation (S4) and the use of heat from biogas co-generation (S5). Fig. 6c reveals that S4 performs better than S3 in sustainability because the environmental burdens of heat are allocated between electricity and heat in the co-generation. S5 demonstrates the significant reduction in GWP (0.19 kg CO_2 eq. per kg) but at the expense of other impacts, notably ODP, PMFP, and TAP (Fig. S9†) mainly due to the fugitive emissions from the

Table 2 Scenario assumptions and TEA and LCA results of S0–S3

Assumptions	MSP ($ per kg bio-catechol)	Energy efficiency (%)	GWP (kg CO_2 eq. per kg)
Baseline scenario (S0)	8.16	61	5.90
CHP with natural gas imported (S1)	4.51	64	2.83
CHP with natural gas imported and PSA (S2)	3.41	64	3.18
Heat imported (S3)	2.02	67	1.58

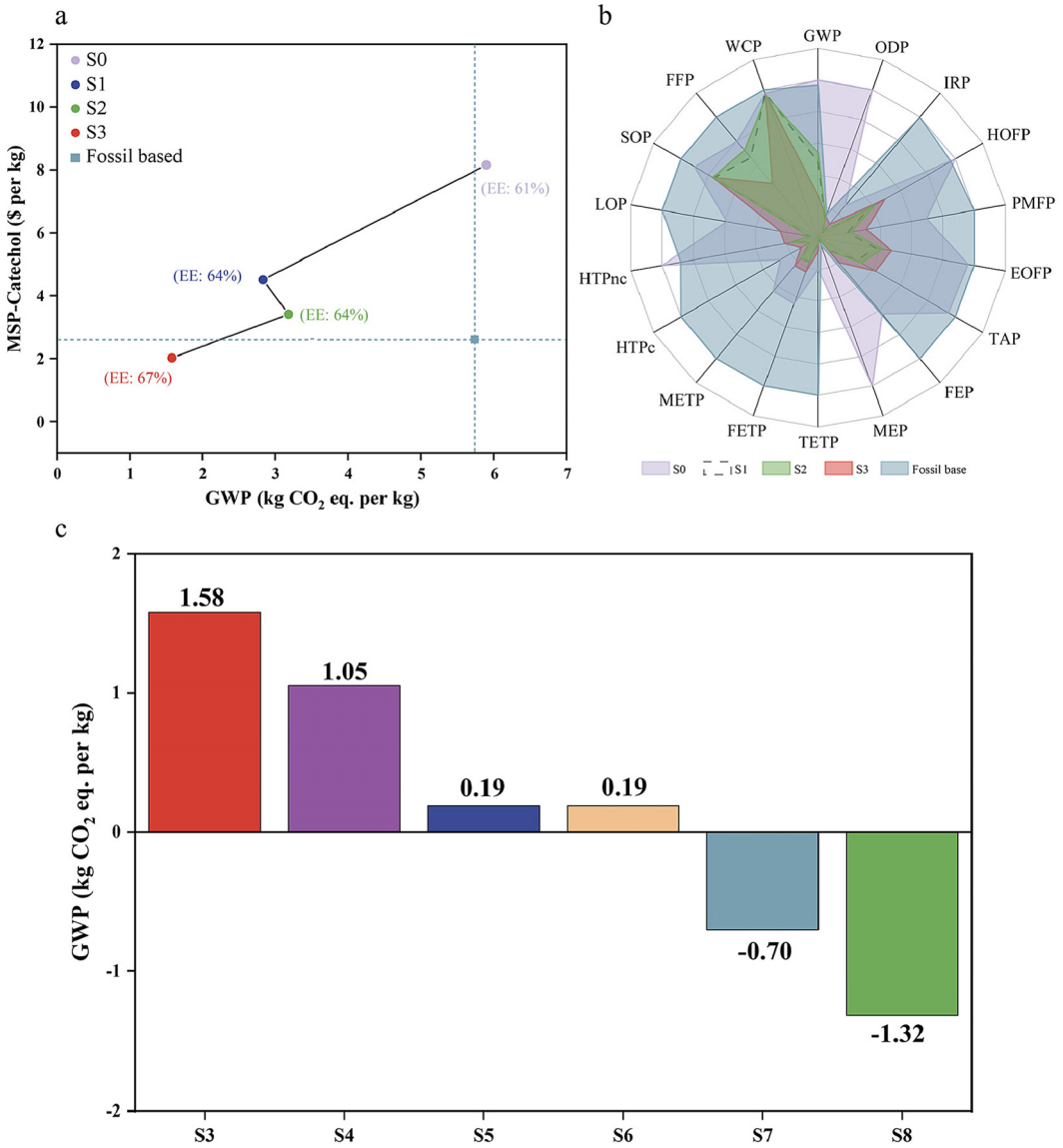

Fig. 6 Comprehensive comparison of techno-economic and life cycle assessment metrics and further optimization of sustainability. (a) Global warming potential (GWP) *vs.* minimum selling price (MSP) of the bio-catechol for S0–S3 and fossil-based scenario. (b) Full LCA analysis results of S0–S3 and fossil-based scenario. (c) GWP results of S3–S8.

anaerobic digestion process and higher emission of SO_2 from biogas combustion. Furthermore, though the distribution of biogas is possible through the existing natural gas pipeline system, the economic feasibility of biogas plants is still a challenge due to the widespread nature of organic resources. The use of virtual pipeline technology can enhance biogas feasibility for industrial applications.[55] Other renewable sources are also considered (Fig. 6c). Based on S5, we substitute fossil-based methanol with bio-methanol, which is produced from biomass synthetic gas (S6). Due to the small consumption of methanol, GWP in S6 is nearly identical to that in S5. In S7, solar electricity is used and the calculated GWP in S7 is −0.70, indicating a net consumption of CO_2, that is, a net carbon capturing effect for the production of bio-catechol. Finally, fossil-based hydrogen is replaced by green hydrogen (electrolysis hydrogen), resulting in a further reduction in GWP to −1.32 kg CO_2 eq. per kg. Overall, given the economic feasibility and GHG reduction potentials of our catechol production technology, the proposed C-lignin biorefinery could contribute to the achievement of a sustainable waste-to-resource circular economy.[56]

4. Conclusion

In order to evaluate the potential of replacing fossil-derived catechol with bio-catechol produced by a C-lignin biorefinery, a conceptual biorefinery plant that can convert waste castor

seed coats into high value-added products, such as catechol, pulp, oligomers and propylene, was constructed and evaluated using techno-economic and life cycle assessments for a comparison with fossil-derived catechol. A series of scenarios were investigated including altering the ways of dealing with solid streams, the implementation of PSA to recycle hydrogen and the supply of heat; bio-catechol could achieve a minimum selling price of $2.02 per kg and a GWP of 1.58 kg CO_2 eq. per kg, both lower than those of fossil-based catechol. The carbon efficiency of this system is about 80%, aligning with green chemistry principles. Overall, this study contributes to the understanding of the environmental and economic performance of a waste castor seed coat conceptual biorefinery plant and paves the way for promoting the utilization of C-lignin from other *Euphorbiaceae* biomass feedstocks (*e.g.*, Chinese tallow, castor, Jatropha, candlenut, and tung). Future research should focus on pilot scale validation of the optimized scenarios to further validate the feasibility of this biorefinery concept, as well as the exploration of advanced catalysts to enhance yield, which could further improve the overall efficiency and economic viability of the process.

Author contributions

Pu Wang: investigation, validation, data curation, visualization, formal analysis, methodology, and writing – original draft; Shihao Su: validation, data curation, methodology, and writing – original draft; Shuizhong Wang: validation, data curation, and writing – original draft; Dexin Zhang: methodology, validation, and visualization; Yuhe Liao: data curation and writing – review & editing; Guoyong Song: resources and writing – review & editing; Lei Wang: conceptualization, funding acquisition, project administration, resources, validation, supervision, conceptualization, and writing – review & editing.

Data availability

Data will be made available on request.

Conflicts of interest

The authors declare that they have no known competing financial interests or personal relationships that could have appeared to influence the work reported in this paper.

Acknowledgements

This work was supported by the National Natural Science Foundation of China (22378333 and 22408294) and the Zhejiang Provincial Department of Science and Technology (2023SDXHDX0006). We acknowledge the Westlake Education Foundation, the Research Center for Industries of the Future at Westlake University for support and thank the Westlake Center for Micro/Nano Fabrication, the Instrumentation and Service Center for Molecular Sciences and the Instrumentation and Service Center for Physical Sciences (ISCPS), Westlake University.

References

1 L. Zhang and X. Sun, *Waste Manage.*, 2018, **77**, 435–446.
2 Y. Duan, A. Pandey, Z. Zhang, M. K. Awasthi, S. K. Bhatia and M. J. Taherzadeh, *Ind. Crops Prod.*, 2020, **153**, 112568.
3 O. Ruíz-Carmona, J. M. Islas-Samperio, L. Larrondo-Posadas, F. Manzini, G. K. Grande-Acosta and C. Álvarez-Escobedo, *Energies*, 2021, **14**, 6560.
4 S. Guo, Z. Wang, G. Chen, M. Zhang, T. Sun, Q. Wang, Z. Du, Y. Chen, M. Wu, Z. Li, T. Lei, K. R. G. Burra and A. K. Gupta, *Process Saf. Environ. Prot.*, 2023, **177**, 380–390.
5 M. R. Patel and N. L. Panwar, *Resour. Conserv. Recycl. Adv.*, 2023, **19**, 200173.
6 Z.-X. Xu, X.-Q. Ma, Y.-Q. Shan, X. Hu, S. M. Osman, J.-J. Liao, P.-G. Duan and R. Luque, *ACS Sustainable Chem. Eng.*, 2022, **10**, 3335–3345.
7 V. Inyang, O. T. Laseinde and G. M. Kanakana, *Int. J. Low-Carbon Technol.*, 2022, **17**, 900–909.
8 J. Tian, F. Yu, Z. Guo, Y. Yan, Y. Xie, Z. Ma, Q. Li, F. Fousseni and W. Liu, *Resour., Conserv. Recycl.*, 2023, **198**, 107157.
9 H. Shao, H. Zhao, J. Xie, J. Qi and T. F. Shupe, *Int. J. Polym. Sci.*, 2019, **2019**, 7231263.
10 C. Siol, D. Thrän and S. Majer, *Biomass Bioenergy*, 2023, **174**, 106839.
11 A. Thorenz, L. Wietschel, D. Stindt and A. Tuma, *J. Cleaner Prod.*, 2018, **176**, 348–359.
12 Q. Liu, T. Kawai, Y. Inukai, D. Aoki, Z. Feng, Y. Xiao, K. Fukushima, X. Lin, W. Shi, W. Busch, Y. Matsushita and B. Li, *Nat. Commun.*, 2023, **14**, 4866.
13 S. Su, L.-P. Xiao, X. Chen, S. Wang, X.-H. Chen, Y. Guo and S.-R. Zhai, *ChemSusChem*, 2022, **15**, e202200365.
14 L. Jiang, C.-G. Wang, P. L. Chee, C. Qu, A. Z. Fok, F. H. Yong, Z. L. Ong and D. Kai, *Sustainable Energy Fuels*, 2023, **7**, 2953–2973.
15 V. K. Garlapati, A. K. Chandel, S. P. J. Kumar, S. Sharma, S. Sevda, A. P. Ingle and D. Pant, *Renewable Sustainable Energy Rev.*, 2020, **130**, 109977.
16 F. Brienza, K. Van Aelst, F. Devred, D. Magnin, B. F. Sels, P. A. Gerin, I. Cybulska and D. P. Debecker, *ACS Sustainable Chem. Eng.*, 2022, **10**, 11130–11142.
17 A. Adler, I. Kumaniaev, A. Karacic, K. R. Baddigam, R. J. Hanes, E. Subbotina, A. W. Bartling, A. J. Huertas-Alonso, A. Moreno, H. Håkansson, A. P. Mathew, G. T. Beckham and J. S. M. Samec, *Joule*, 2022, **6**, 1845–1858.
18 S. Su, C. Wu and L. Wang, *Ind. Crops Prod.*, 2024, **222**, 119974.
19 Y. Li, L. Shuai, H. Kim, A. H. Motagamwala, J. K. Mobley, F. Yue, Y. Tobimatsu, D. Havkin-Frenkel, F. Chen,

R. A. Dixon, J. S. Luterbacher, J. A. Dumesic and J. Ralph, *Sci. Adv.*, 2018, **4**(eaau2968).
20 S. Wang, S. Su, L.-P. Xiao, B. Wang, R.-C. Sun and G. Song, *ACS Sustainable Chem. Eng.*, 2020, **8**, 7031–7038.
21 S. Su, S. Wang and G. Song, *Green Chem.*, 2021, **23**, 7235–7242.
22 S. Su, Q. Shen, S. Wang and G. Song, *Int. J. Biol. Macromol.*, 2023, **239**, 124256.
23 K. Barta, G. R. Warner, E. S. Beach and P. T. Anastas, *Green Chem.*, 2014, **16**, 191–196.
24 M. L. Stone, E. M. Anderson, K. M. Meek, M. Reed, R. Katahira, F. Chen, R. A. Dixon, G. T. Beckham and Y. Román-Leshkov, *ACS Sustainable Chem. Eng.*, 2018, **6**, 11211–11218.
25 C. Liu, S. Wang, B. Wang and G. Song, *Ind. Crops Prod.*, 2021, **169**, 113666.
26 S. Wang, K. Zhang, H. Li, L.-P. Xiao and G. Song, *Nat. Commun.*, 2021, **12**, 416.
27 M. Nar, H. R. Rizvi, R. A. Dixon, F. Chen, A. Kovalcik and N. D'Souza, *Carbon*, 2016, **103**, 372–383.
28 Z.-M. Zhao, X. Meng, Y. Pu, M. Li, Y. Li, Y. Zhang, F. Chen and A. J. Ragauskas, *Biomacromolecules*, 2023, **24**, 3996–4004.
29 F. Liu, X. Dong, X. Zhao and L. Wang, *Energy Convers. Manage.*, 2021, **246**, 114653.
30 B. Pang, Z. Sun, L. Wang, W.-J. Chen, Q. Sun, X.-F. Cao, X.-J. Shen, L. Xiao, J.-L. Yan, P. J. Deuss, T.-Q. Yuan and R.-C. Sun, *Chem. Eng. J.*, 2021, **419**, 129565.
31 A. W. Bartling, M. L. Stone, R. J. Hanes, A. Bhatt, Y. Zhang, M. J. Biddy, R. Davis, J. S. Kruger, N. E. Thornburg, J. S. Luterbacher, R. Rinaldi, J. S. M. Samec, B. F. Sels, Y. Román-Leshkov and G. T. Beckham, *Energy Environ. Sci.*, 2021, **14**, 4147–4168.
32 W. Arts, K. Van Aelst, E. Cooreman, J. Van Aelst, S. Van den Bosch and B. F. Sels, *Energy Environ. Sci.*, 2023, **16**, 2518–2539.
33 Y. Liao, S.-F. Koelewijn, G. Van den Bossche, J. Van Aelst, S. Van den Bosch, T. Renders, K. Navare, T. Nicolaï, K. Van Aelst, M. Maesen, H. Matsushima, J. M. Thevelein, K. Van Acker, B. Lagrain, D. Verboekend and B. F. Sels, *Science*, 2020, **367**, 1385–1390.
34 A. Mabrouk, X. Erdocia, M. G. Alriols and J. Labidi, *J. Cleaner Prod.*, 2018, **198**, 133–142.
35 M. Montazeri and M. J. Eckelman, *ACS Sustainable Chem. Eng.*, 2016, **4**, 708–718.
36 Tongliao Tonghua Ricinus Chemical Co., Ltd, **https://thbmhgjt.company.lookchem.cn/**.
37 Inner Mongolia Tianrun Castor Development Co., Ltd, **https://www.agronet.com.cn/c/526249/CompanyProfile.html**.
38 R. D. D. Humbird, L. Tao, C. Kinchin, D. Hsu, A. Aden, P. Schoen, J. Lukas, B. Olthof, M. Worley, D. Sexton and D. Dudgeon, *Process Design and Economics for Biochemical Conversion of Lignocellulosic Biomass to Ethanol Dilute-Acid Pretreatment and Enzymatic Hydrolysis of Corn Stover*, 2011.
39 A. Dutta, A. Sahir, E. Tan, D. Humbird, L. J. Snowden-Swan, P. Meyer, J. Ross, D. Sexton, R. Yap and J. Lukas, *Process Design and Economics for the Conversion of Lignocellulosic Biomass to Hydrocarbon Fuels Thermochemical Research Pathways with In Situ and Ex Situ Upgrading of Fast Pyrolysis Vapors*, 2015.
40 L. T. R. Davis, E. C. D. Tan, M. J. Biddy, G. T. Beckham and C. Scarlata, *Process Design and Economics for the Conversion of Lignocellulosic Biomass to Hydrocarbons: Dilute-Acid and Enzymatic Deconstruction of Biomass to Sugars and Biological Conversion of Sugars to Hydrocarbons*, 2013.
41 M. Tschulkow, T. Compernolle, S. Van den Bosch, J. Van Aelst, I. Storms, M. Van Dael, G. Van den Bossche, B. Sels and S. Van Passel, *J. Cleaner Prod.*, 2020, **266**, 122022.
42 D. Mignard, *Chem. Eng. Res. Des.*, 2014, **92**, 285–294.
43 J. B. V. Bastos, J. G. S. S. Maia, S. Borschiver, A. Szklo and A. R. Secchi, *J. Cleaner Prod.*, 2022, **337**, 130585.
44 ISO, 2000. ISO 2000: ISO 14042, Environmental management – Life cycle assessment - Life cycle impact assessment.
45 ISO, 2006. ISO 2006: ISO 14040, Environmental management – Life cycle assessment - Principles and framework.
46 Anhui Yiyi New Materials Co., Ltd, Project: Annual Production of 15 000 Tons of Catechol (1,2-Dihydroxybenzene)/Hydroquinone (1,4-Dihydroxybenzene) and 5000 Tons of Guaiacol (o-Methoxyphenol)/p-Methoxyphenol;2023-06-25;091156 (1), **https://www.zbwmy.com/162/163/2023/08/24/103138321.html**.
47 ReCiPe, 2016., **https://pre-sustainability.com/articles/recipe/**.
48 S. A. Channiwala and P. P. Parikh, *Fuel*, 2002, **81**, 1051–1063.
49 B. H. A. Sluiter, R. Ruiz, C. Scarlata, J. Sluiter, D. Templeton and D. Crocker, *Determination of Structural Carbohydrates and Lignin in Biomass*, 2008.
50 Chinabgao, **https://m.chinabgao.com/jiage/17477773.html**.
51 G. Li, K. Li, S. Ma and Y. Zhang, *J. Cleaner Prod.*, 2023, **416**, 137988.
52 GB 16889-2024, **https://www.mee.gov.cn/ywgz/fgbz/bz/bzwb/gthw/gtfwwrkzbz/202408/t20240809_1083681.shtml**.
53 GB 16297-1996, **https://www.mee.gov.cn/ywgz/fgbz/bz/bzwb/dqhjbh/dqgdwrywrwpfbz/199701/t19970101_67504.htm**.
54 D. Che, Y. Liu and C. Gao, *Energy Convers. Manage.*, 2004, **45**, 3251–3266.
55 . D. Ó. Céileachair, S. O'Callaghan, D. M. Wall, D. Goulding, D. O'Connor, J. D. Murphy and R. O'Shea, *J. Cleaner Prod.*, 2023, **407**, 137075.
56 J. Sherwood, *Bioresour. Technol.*, 2020, **300**, 122755.